This article was published in Chemical Engineering Science, 126, 440-445, 2015
http://dx.doi.org/10.1016/j.ces.2014.12.054

Micro and macro flow systems to study *Escherichia coli* adhesion to biomedical materials

Moreira JMR[a], Ponmozhi J[b], Campos JBLM[b], Miranda JM[b], Mergulhão FJ[a]

[a] LEPABE – Department of Chemical Engineering, Faculty of Engineering, University of Porto, Rua Dr. Roberto Frias s/n 4200-465 Porto, Portugal

[b] CEFT – Department of Chemical Engineering, Faculty of Engineering, University of Porto, Rua Dr. Roberto Frias s/n 4200-465 Porto, Portugal

Correspondent author: Filipe J. M. Mergulhão, Chemical Engineering Department, Faculty of Engineering University of Porto, Rua Dr. Roberto Frias, 4200-465 Porto, Portugal. Phone: (+351) 225081668. Fax: (+351) 5081449. E-mail: filipem@fe.up.pt.

Abstract

Micro and macro flow systems have been used as *in vitro* platforms to study bacterial adhesion under physiological conditions. The decision of which platform to use has been dictated by the dimensions of the *in vivo* systems that they are supposed to mimic and by the available resources in each laboratory. In this work, a microchannel and a parallel plate flow chamber were operated in order to observe the adhesion of *Escherichia coli* to different materials that are commonly used to construct biomedical devices for the urinary and reproductive systems. The surface properties of cellulose acetate, glass, poly-L-lactide, and polydimethylsiloxane were thermodynamically characterized by contact angle measurement and the flow along the platforms was simulated by computational fluid dynamics. The results presented in this study demonstrate that different adhesion rates were obtained on different materials but similar values were obtained in the micro and macro platforms for each material under the same shear stress (0.022 Pa). This suggests that despite the scale factor (80x) both platforms may be equally used to mimic the same biomedical biofilms for a specified shear stress. Thus, depending on the expertise and equipment availability in different labs, micro flow systems can be used taking advantage of lower hold-up volumes or macro flow systems can be selected in order to obtain a higher biofilm mass which can be used for further biochemical analysis.

Keywords: Adhesion, *Escherichia coli,* microchannel, parallel plate flow chamber, biomedical materials

1. Introduction

Biofilms are communities of microorganisms adhered to living or inert surfaces, surrounded by

50 self-produced extracellular polymeric substances (Stoodley et al., 2002). Microbial adhesion to
51 surfaces is dictated by a set of important variables, including cell transport and the imposed shear
52 stress, which are affected by the flow conditions, and by physicochemical interactions between
53 cells and surfaces (Pace et al., 2006).
54 Hospital-acquired infections are the fourth leading cause of death in the U.S and 65% of this
55 infections are caused by biofilms (Robert and Salek, 2010). Most cases of infection in critically ill
56 patients are associated with medical devices. Infection rates in medical devices comprise dental
57 implants and fracture fixation devices (5-10%), bladder catheters (10-30%) and heart assistant
58 devices (25-50%) (Weinstein and Darouiche, 2001). *Escherichia coli* has been documented as the
59 major cause for infection of these devices (Castonguay et al., 2006). This bacteria is responsible
60 for 80% of the urinary tract infections, 1.5% of infections in breast implants and it has also been
61 found in pacemakers and contact lenses (Shunmugaperumal, 2010; Trautner and Darouiche, 2004;
62 Wood, 1999). Bacterial adhesion and biofilm development on the surface of these medical devices
63 can compromise their function and increase the health risk (Weinstein and Darouiche, 2001).
64 The scientific community has been trying to understand how to control biofilms in order to reduce
65 their effects. Bacterial adherence to a surface is one of the first steps in biofilm formation (Nikolaev
66 and Plakunov, 2007) and controlling this step is one of the most promising biofilm control
67 strategies (Campoccia et al., 2013; Chen and Zhu, 2005; Gallardo-Moreno et al., 2011; Petrova
68 and Sauer, 2012). Shumi et al. (2013) used a microfluidic device in order to investigate the
69 influence of flow shear stress and sucrose concentration in the adhesion of *Streptococcus mutans*
70 aggregates. With this platform they simulated the space between adjacent teeth in order to
71 understand the process of dental caries formation by *S. mutans*. They observed that sucrose-
72 dependent aggregates (larger than 50 μm in diameter) are more tolerant to shear stress than sucrose-

73 independent aggregates. Bruinsma et al. (2001) investigated the effect of physicochemical surface
74 interactions between seven different bacterial strains isolated from ophthalmic infections and
75 hydrophilic and hydrophobic contact lenses (CL) with and without an adsorbed tear film. They
76 used a parallel plate flow chamber (PPFC) for bacterial adhesion assays in order to mimic the
77 natural eye environment and understand the process of microbial keratitis development. They
78 concluded that CL hydrophobicity dictates the composition of the adsorbed tear film and thus the
79 extension of bacterial adhesion to the lens. Andersen et al. (2010) have used a flow chamber
80 operated at hydrodynamic flow conditions similar to those found in implanted devices in order to
81 observe the effect of surface chemistry and temperature in adhesion and biofilm formation by *E.*
82 *coli* strains on two types of silicone rubber. They observed that surface chemistry influenced
83 surface colonization and that temperature was also a critical factor.
84 PPFCs and microchannels are two of the most widely used flow devices for adhesion/biofilm
85 studies (Busscher and van der Mei, 2006; Gottenbos et al., 1999; Rivet et al., 2011). Both systems
86 enable real-time visualization of bacterial adhesion/biofilm development in conditions which
87 mimic *in vivo* environments (Barros et al., 2013; Kim et al., 2012). They enable control of the
88 hydrodynamic conditions (*e.g.* shear stress), temperature, testing different materials and they can
89 be used as high-throughput platforms (Bakker et al., 2003; Barros et al., 2013; Salta et al., 2013;
90 Situma et al., 2006). Microfluidic systems have some advantages such as low volume requirements
91 (*e.g.* reagents) which may lead to reduced operational costs (Situma et al., 2006), they mimic
92 phenomena occurring at a microscale, such as in microfluidic drug delivery systems (Gerecht et
93 al., 2013), and due to their small dimensions they are easy to handle (Aimee et al., 2013). On the
94 other hand, this platform is not accessible to many labs due to the unique requirements of micro-
95 fabrication processes, liquid handling and sampling. These techniques are often time-consuming,

96 labor-intensive and expensive since in most cases microchannels cannot be reused (Situma et al.,
97 2006). Fabrication of a common PPFC can be more straightforward for some labs with the added
98 advantage that after fabrication it can be used indefinitely. Additionally, several materials can be
99 tested at the same time or consecutively and the amount of produced biofilm is higher enabling
100 further biochemical analysis. This platform is often used to mimic systems with dimensions larger
101 than few centimeters (Teodósio et al., 2013). The selection of a platform for bacterial adhesion
102 studies can be an intricate issue. Both systems have their relative advantages and disadvantages
103 and their selection is usually dictated by the equipment/expertise existing in the lab as well by the
104 similarity to the physiological system that is supposed to be mimicked (*e.g.* size similarity) (Aimee
105 et al., 2013; Bakker et al., 2003; Barros et al., 2013; Gerecht et al., 2013; Teodósio et al., 2013).
106 In this work, *E. coli* adhesion was visualized in a microchannel and in a PPFC in order to compare
107 two platforms commonly used in adhesion studies. The same average wall shear stress (0.022 ±
108 0.002 Pa) was used on both systems and similar shear stress values can be found in the urinary
109 (Aprikian et al., 2011) or reproductive systems (Nauman et al., 2007). Three materials, cellulose
110 acetate (CA), poly-L-lactide (PLLA), and polydimethylsiloxane (PDMS), which are currently used
111 to fabricate biomedical devices that are inserted in these body locations and a glass (used as a
112 control) were tested (Abbasi et al., 2001; Andersson, 2006; Grewe et al., 2011; Multanen et al.,
113 2000). The main objective of this work was to evaluate if the size similarity between the *in vitro*
114 formation platform and the *in vivo* scenario is a relevant issue in the selection of the most adequate
115 biofilm formation platform.
116
117 **2. Materials and methods**
118 2.1 Numerical simulations

Numerical simulations were made in Ansys Fluent CFD package (version 14.5). A model of each system was built in Design Modeller 14.5 and was discretized by Meshing 14.5.

The mesh for the PPFC (1 694 960 hexahedral cells) was refined near the walls, where velocity gradients are higher. A refined cylindrical core was also introduced to improve the accuracy of the calculation of the jet flow that forms at the inlet of the PPFC. Results were obtained by solving the SST k-ω turbulent model (Menter, 1994) with low Reynolds corrections. The velocity-pressure coupled equations were solved by the PISO algorithm (Issa, 1986), the QUICK scheme (Leonard, 1979) was used for the discretization of the momentum equations and the PRESTO! scheme for pressure equation discretization. The no slip boundary condition was considered for all the bounded walls. The SST k-ω turbulent model with low Reynolds corrections was selected because the flow conditions in the PPFC indicate the presence of regions with low Reynolds turbulence. While the Reynolds number in the inlet is 3600 (and therefore turbulence can develop in this region) the Reynolds number in the viewing area is 346. Turbulence decreases along the chamber, and the flow can even become laminar. Simulations using the SST k-ω model were compared to those obtained by solving the Navier-Stokes equations for the laminar regime and the results in the viewing area were similar. Shear stresses of 0.024 and 0.021 Pa were obtained with the SST k-ω model and for the laminar case, respectively.

The mesh for the microfluidic channel was divided into two parts, an inlet region with 124 154 hexahedral cells and the microchannel with a mesh of 94 374 hexahedral cells uniformly distributed. Results were obtained by solving the Navier-Stokes equations for the laminar regime using the PISO algorithm, the QUICK scheme and PRESTO!.

For the simulations, the initial velocity field was set to zero, a uniform velocity profile was set at the inlet and the pressure was set to zero at the outlet. The properties of water (density and

viscosity) at 37 ºC were used for the fluid. Simulations were made in transient mode, to assure convergence and to capture transient flow structures. For each case, 2 s of physical time were simulated with a fixed time step of 10^{-4} s.

2.2 Bacteria and culture conditions

Escherichia coli JM109(DE3) was used since this strain had already demonstrated a good biofilm formation capacity (Teodósio et al., 2012). A starter culture was obtained by inoculation of 500 μL of a glycerol stock (kept at -80 ºC) to a total volume of 0.2 L of inoculation media with 5.5 g L^{-1} glucose, 2.5 g L^{-1} peptone, 1.25 g L^{-1} yeast extract in phosphate buffer (1.88 g L^{-1} KH_2PO_4 and 2.60 g L^{-1} Na_2HPO_4) at pH 7.0, as described by Teodósio et al. (2011). This culture was grown in a 1 L shake-flask, incubated overnight at 37 ºC with orbital agitation (120 rpm). A volume of 60 mL from the overnight grown culture was used to harvest cells by centrifugation (for 10 min at 3202 *g*). Cells were washed twice with citrate buffer 0.05 M (Simões et al., 2008), pH 5.0 and finally the pellet was resuspended and diluted in the same buffer in order to reach a cell concentration of $7.6x10^7$ cell.mL^{-1}.

2.3 Surface preparation

Three polymers (CA, PDMS, PLLA) and glass, used in this study for comparative purposes, were prepared for adhesion assays. Glass slides commercially available (VWR) were firstly washed with a commercial detergent (Sonasol Pril, Henkel Ibérica S A) and immersed in sodium hypochlorite (3%). After rinsing with distilled water, part of the glass slides was coated with the polymers. Coatings were prepared by mixing the polymer in solid form with solvents. Dichloromethane was added to PLLA at 5% (w/w), acetone was added to CA at 8% (w/w), and a

165 curing agent (Sylgard 184 Part B, Dow Corning) was added (at a 1:10 ratio) to PDMS (polymers
166 from Sigma, solvents from Normapur). These mixtures were carefully stirred to homogenize the
167 two components without introducing bubbles. The polymers were then deposited as a thin layer
168 (average thickness of 10 µm) on the top of glass slides by spin coating (Spin150 PolosTM).
169
170 2.4 Surface characterization
171 Bacterial and surface hydrophobicity was evaluated considering the Lifshitz van der Waals acid
172 base approach (van Oss, 1994). The contact angles were determined automatically by the sessile
173 drop method in a contact angle meter (OCA 15 Plus; Dataphysics, Filderstadt, Germany) using
174 water, formamide and α-bromonaphtalene (Sigma) as reference liquids. The surface tension
175 components of the reference liquids were taken from literature (Janczuk et al., 1993). For each
176 surface, at least 10 measurements with each liquid were performed at 25 ± 2 ºC. One *E. coli*
177 suspension was prepared in the same conditions as for the adhesion assays and its physicochemical
178 properties were also determined by sessile drop contact angle measurement as described by
179 Busscher et al. (1984).
180 The model proposed by van Oss (1994) indicates that the total surface energy (γ^{Tot}) of a pure
181 substance is the sum of the Lifshitz van der Waals components of the surface free energy (γ^{LW})
182 and Lewis acid-base components (γ^{AB}):
183 $$\gamma^{Tot} = \gamma^{\mathrm{LW}} + \gamma^{\mathrm{AB}} \quad (1)$$
184 The polar AB component comprises the electron acceptor γ^{+} and electron donor γ^{-} parameters,
185 and is given by:
186 $$\gamma^{\mathrm{AB}} = 2\sqrt{\gamma^{+}\gamma^{-}} \quad (2)$$

The surface energy components of a solid or bacterial surface (s) are obtained by measuring the contact angles (θ) with the three different liquids (l) with known surface tension components, followed by the simultaneous resolution of three equations of the type:

$$(1+\cos\theta)\gamma_l = 2\left(\sqrt{\gamma_s^{LW}\gamma_l^{LW}} + \sqrt{\gamma_s^{+}\gamma_l^{-}} + \sqrt{\gamma_s^{-}\gamma_l^{+}}\right) \quad (3)$$

The degree of hydrophobicity of a given surface (solid or bacterial surface) is expressed as the free energy of interaction (ΔG mJ.m^{-2}) between two entities of that surface immersed in a polar liquid (such as water (w) as a model solvent). ΔG was calculated from the surface tension components of the interacting entities, using the equation:

$$\Delta G = -2\left(\sqrt{\gamma_s^{LW}} - \sqrt{\gamma_w^{LW}}\right)^2 + 4\left(\sqrt{\gamma_s^{+}\gamma_w^{-}} + \sqrt{\gamma_s^{-}\gamma_w^{+}} - \sqrt{\gamma_s^{+}\gamma_s^{-}} - \sqrt{\gamma_w^{+}\gamma_w^{-}}\right); \quad (4)$$

If the interaction between the two entities is stronger than the interaction of each entity with water, $\Delta G < 0$ mJ.m^{-2}, the material is considered hydrophobic, if $\Delta G > 0$ mJ.m^{-2}, the material is hydrophilic.

2.5 PPFC experiments

A PPFC with dimensions of 16 x 254 x 8 mm (W x L x H) was coupled to a jacketed tank connected to a centrifugal pump by a tubing system to conduct the adhesion assay (Moreira et al., 2014). The PPFC contained a bottom and a top opening for the introduction of the test surfaces. The PPFC was mounted in a microscope (Nikon Eclipse LV100, Japan) to monitor the *E. coli* attachment to each surface for 30 min. The cellular suspension was circulated at 4 mL.s^{-1} and images were acquired every 60 s with a camera (Nikon digital sight DS-RI 1, Japan) connected to the microscope. The temperature was kept constant at 37 ºC using a recirculating water bath. All adhesion experiments were performed in triplicate for each surface.

209

210 2.6 Microchannel experiments

211 Molds were prepared by the xurographic technique (Bartholomeusz et al., 2005) to fabricate
212 PDMS microchannels with dimensions of 0.45 x 15 x 0.10 mm (W x L x H) by standard PDMS
213 soft lithography (Duffy et al., 1998). The microchannels were placed and sealed over glass slides
214 coated in a two-step procedure. On the first step, the different polymers were prepared and
215 deposited as a thin layer in the glass slides by spin coating as described in the surface preparation
216 section. Then, a mask was placed in the visualization zone (to protect the polymeric surface) and
217 a second coating, with PDMS, was deposited by spin coating. The mask was removed exposing
218 the polymeric surface surrounded by PDMS. Sealing was assured by PDMS-PDMS bonding (after
219 20 minutes of partial curing), without the use of oxygen plasma. Then the microchannel was
220 coupled to a syringe pump by a tubing system to conduct the adhesion assay. The microchannel
221 was mounted in a microscope (Leica DMI 5000 M) to monitor the *E. coli* attachment to each
222 surface for 30 min. The cellular suspension was circulated at 0.02 $\mu L.s^{-1}$ and images were acquired
223 every 60 s with a camera (Leica DFC350 FX) connected to the microscope. The temperature was
224 kept constant at 37 ºC by a hot air atmosphere around the microchannel using a hot air blower. All
225 adhesion experiments were performed in triplicate for each surface.

226

227 2.7 Data analysis

228 The microscopy images recorded during the on-line cell adhesion assays were analyzed with an
229 image analysis and measurement software program (ImageJ 1.46r) in order to obtain the number
230 of adhered cells over time (30 min assay). This program was also used to calibrate the size of the
231 field of view of each image so that pixels could be converted to square centimeters. The number

of bacterial cells was then divided by the surface area of the field of view to obtain the density of bacteria per square centimeter. This cell density was plotted along the assay time and the adhesion rate (cells.cm^{-2}.s^{-1}) was calculated from the slope of a linear regression of the data obtained for each surface and platform. Images taken at the endpoint of the assay were used to calculate the surface coverage using the same software.

2.8 Statistical analysis

Paired *t*-test analyses were performed to evaluate if statistically significant differences were obtained between the two platforms for each material and between different materials on the same platform. Three independent experiments were performed for each surface and platform. Each time point was evaluated individually using the three independent results obtained with one surface in the PPFC and the three individual results obtained with the same surface in the microchannel. Results were considered statistically different for a confidence level greater than 95% ($P < 0.05$). Standard deviation between the three values obtained from the independent experiments was also calculated and indicated as error bars.

3. Results and discussion

Figure 1 a) depicts the wall shear stress distribution along the PPFC. The highest wall shear stress values are obtained in the entry zone for $x < 0.05$ m and afterwards flow stabilizes as it approaches the viewing area where the conditions are of steady flow. Figure 1 b) shows the wall shear stress for the microchannel. The inlet region, which is used for micro/macro interfacing, has a very low shear stress and no developing region is observed. In figure 2 it is possible to observe that the wall shear stress along the *x*-axis shows one peak close to the entry in the PPFC. Regarding the

255 microchannel, the wall shear stress is constant along the flow direction. Both figures show that the
256 wall shear stress is constant in the region where adhesion was measured (marked as viewing area)
257 and that the average shear stress was the same on both platforms (0.022 ± 0.002 Pa) corresponding
258 to a shear rate of 32 s^{-1}.
259 In table 1 it is possible to observe that these systems have very different section areas. Also, the
260 microchannel has a higher aspect ratio when compared to the PPFC and the height of the PPFC is
261 80x higher than in the microchannel. Different flow rates were operated in each system in order to
262 obtain identical average wall shear stresses. Approximate shear stresses can be found in different
263 locations of the human body like in the bladder, urethra (Aprikian et al., 2011) and uterus (Nauman
264 et al., 2007). Three materials (CA, PLLA and PDMS) commonly used in biomedical devices
265 (Abbasi et al., 2001; Andersson, 2006; Grewe et al., 2011; Multanen et al., 2000) which can be
266 applied in these body locations and glass (for control purposes) were chosen for bacterial adhesion
267 assays. A physicochemical characterization of these materials was made by contact angle
268 measurement. In table 2 it is possible to observe that glass is a hydrophilic surface, whereas all the
269 other tested surfaces are hydrophobic, although with different degrees of hydrophobicity.
270 Additionally it is also verified that *E. coli* has a hydrophilic surface.
271 Figure 3 depicts the adhesion curves obtained for each material (PDMS, PLLA, CA and glass) in
272 the PPFC and in the microchannel. The number of adhered cells increased with time in all cases.
273 It is also possible to observe that the number of adhered cells on a given surface was similar on
274 both platforms ($P > 0.05$) and that this was observed for more than 90% of the time points.
275 Additionally, in table 1 it is also possible to observe that a similar maximum surface coverage was
276 achieved (for glass) and similar values for each surface were obtained in the macro and micro
277 systems (data not shown).

278 In figure 4 it is possible to observe the adhesion rates for each tested material obtained in the
279 microchannel and in the PPFC. It is possible to verify that different adhesion rates were obtained
280 on the different materials and that similar adhesion rates were obtained on glass and PDMS ($P >$
281 0.05). The highest adhesion rate was obtained on glass and PDMS and the lowest on PLLA ($P <$
282 0.05). A higher adhesion rate was expected in the most hydrophobic surface and the lowest in the
283 hydrophilic glass (Kochkodan et al., 2008). However, a correlation between the bacterial adhesion
284 rates and surface properties was not found for any of the systems. On a previous study using the
285 same strain in adhesion assays performed in static conditions (with silicone, stainless steel,
286 polyvinyl chloride and glass), a correlation between surface thermodynamic properties and
287 adhesion results was obtained (Gomes et al., 2014). Similarly, in a study by Katsikogianni et al.
288 (2008), a correlation between surface thermodynamic properties and *S. epidermidis* adhesion on
289 plasma modified polyethylene terephthalate films was obtained in static conditions. However,
290 when flow was established, at shear rates of 50 and 200 s^{-1}, a correlation could not be found. Thus
291 it seems that the predictability of the thermodynamic theory is somewhat restricted during flow
292 conditions as it may have occurred in the present work. Besides surface thermodynamic properties,
293 several factors are known to influence bacterial adhesion to surfaces including chemical
294 composition of the material, the physical configuration (An and Friedman, 1998) and the presence
295 of specific bacterial components like adhesins which are also determinant on bacterial attachment
296 (Desrousseaux et al., 2013).
297
298 **4. Conclusions**
299 In this work, it was observed that for these flow systems with the same geometry and operated at
300 identical wall shear stresses, the same surface coverage and adhesion rates were obtained despite

the scale factor. It is therefore reasonable to assume that if similar results were obtained in both platforms in these conditions they are capable of mimicking the same biomedical scenarios. Therefore, the results obtained in one of these platforms may be transferable to the other and thus the dimensions of the real systems that they are supposed to mimic may no longer be a limiting parameter in the selection of the most adequate flow system for bacterial adhesion assays. This enables different labs to choose whatever system they prefer due to their expertise and equipment availability taking into consideration the advantages and limitations of each system.

Acknowledgments

The authors acknowledge the financial support provided by Operational Programme for Competitiveness Factors – COMPETE, European Fund for Regional Development – FEDER and by Portuguese Foundation for Science and Technology – FCT through Projects PTDC/EBB-BIO/104940/2008 and PTDC/EQU-FTT/105535/2008.

References

Abbasi, F., Mirzadeh, H., Katbab, A.-A., 2001. Modification of polysiloxane polymers for biomedical applications: a review. Polym Int 50, 1279-1287.

Aimee, K.W., Laura, H., Matthew, R.P., Marvin, W., 2013. Going local: technologies for exploring bacterial microenvironments. Nat Rev Microbiol 11, 337-348.

An, Y.H., Friedman, R.J., 1998. Concise review of mechanisms of bacterial adhesion to biomaterial surfaces. J Biomed Mater Res 43, 338-348.

Andersen, T.E., Kingshott, P., Palarasah, Y., Benter, M., Alei, M., Kolmos, H.J., 2010. A flow chamber assay for quantitative evaluation of bacterial surface colonization used to investigate the

influence of temperature and surface hydrophilicity on the biofilm forming capacity of uropathogenic *Escherichia coli*. J Microbiol Methods 81, 135-140.

Andersson, J.U., 2006. Urinary catheter. Patent.

Aprikian, P., Interlandi, G., Kidd, B.A., Le Trong, I., Tchesnokova, V., Ykovenko, O., Whitfield, M.J., Bullitt, E., Stenkamp, R.E., Thomas, W.E., Sokurenko, E., 2011. The bacterial fimbrial tip acts as a mechanical force sensor. PLoS Biol 9.

Bakker, D.P., van der Plaats, A., Verkerke, G.J., Busscher, H.J., van der Mei, H.C., 2003. Comparison of velocity profiles for different flow chamber designs used in studies of microbial adhesion to surfaces. Appl Environ Microbiol 69, 6280-6287.

Barros, J., Grenho, L., Manuel, C.M., Ferreira, C., Melo, L.F., Nunes, O.C., Monteiro, F.J., Ferraz, M.P., 2013. A modular reactor to simulate biofilm development in orthopedic materials. Int Microbiol 16, 191-198.

Bartholomeusz, D.A., Boutte, R.W., Andrade, J.D., 2005. Xurography: Rapid prototyping of microstructures using a cutting plotter. J Microelectromech Syst 14, 1364-1374.

Bruinsma, G.M., van der Mei, H.C., Busscher, H.J., 2001. Bacterial adhesion to surface hydrophilic and hydrophobic contact lenses. Biomaterials 22, 3217-3224.

Busscher, H., Weerkamp, A., Mei, H.v.d., Pelt, A., Jong, H., Arends, J., 1984. Measurements of the surface free energy of bacterial cell surfaces and its relevance for adhesion. Appl Environ Microbiol 48, 980-983.

Busscher, H.J., van der Mei, H.C., 2006. Microbial adhesion in flow displacement systems. Clin Microbiol Rev 19, 127-141.

Campoccia, D., Montanaro, L., Arciola, C.R., 2013. A review of the clinical implications of anti-infective biomaterials and infection-resistant surfaces. Biomaterials 34, 8018-8029.

347 Castonguay, M.H., van der Schaaf, S., Koester, W., Krooneman, J., van der Meer, W., Harmsen,
348 H., Landini, P., 2006. Biofilm formation by *Escherichia coli* is stimulated by synergistic
349 interactions and co-adhesion mechanisms with adherence-proficient bacteria. Res Microbiol 157,
350 471-478.
351 Chen, G., Zhu, H., 2005. Bacterial adhesion to silica sand as related to Gibbs energy variations.
352 Colloids Surf B Biointerfaces 44, 41-48.
353 Desrousseaux, C., Sautou, V., Descamps, S., Traoré, O., 2013. Modification of the surfaces of
354 medical devices to prevent microbial adhesion and biofilm formation. J Hosp Infect 85, 87-93.
355 Duffy, D.C., McDonald, J.C., Schueller, O.J.A., Whitesides, G.M., 1998. Rapid prototyping of
356 microfluidic systems in poly(dimethylsiloxane). Anal Chem 70, 4974-4984.
357 Gallardo-Moreno, A.M., Navarro-Pérez, M.L., Vadillo-Rodríguez, V., Bruque, J.M., González-
358 Martín, M.L., 2011. Insights into bacterial contact angles: Difficulties in defining hydrophobicity
359 and surface Gibbs energy. Colloids Surf B Biointerfaces 88, 373-380.
360 Gerecht, S., Abaci, H.E., Drazer, G., 2013. Recapitulating the vascular microenvironment in
361 microfluidic platforms Nano LIFE 03, 1340001.
362 Gomes, L.C., Silva, L.N., Simões, M., Melo, L.F., Mergulhão, F.J., 2014. *Escherichia coli*
363 adhesion, biofilm development and antibiotic susceptibility on biomedical materials. J Biomed
364 Mater Res Part B n/a-n/a.
365 Gottenbos, B., van der Mei, H.C., Busscher, H.J., 1999. Models for studying initial adhesion and
366 surface growth in biofilm formation on surfaces, in: Lorsch, J. (Ed.), Methods in Enzymology.
367 Academic Press, pp. 523-533.
368 Grewe, D., Roeder, B., Charlebois, S., Griebel, A., 2011. Manufacturing methods for covering
369 endoluminal prostheses. Google Patents.

Issa, R.I., 1986. Solution of the implicitly discutised fluid flow equations by operating-splitting. J Comput Phys 62, 40-65.

Janczuk, B., Chibowski, E., Bruque, J.M., Kerkeb, M.L., Gonzales-Caballero, F.J., 1993. On the consistency of surface free energy components as calculated from contact angle of different liquids: an application to the cholesterol surfaces. J Colloid Interface Sci 159, 421-428.

Katsikogianni, M., Amanatides, E., Mataras, D., Missirlis, Y.F., 2008. *Staphylococcus epidermidis* adhesion to He, He/O_2 plasma treated PET films and aged materials: Contributions of surface free energy and shear rate. Colloids Surf B Biointerfaces 65, 257-268.

Kim, J., Park, H.-D., Chung, S., 2012. Microfluidic approaches to bacterial biofilm formation. Molecules 17, 9818-9834.

Kochkodan, V., Tsarenko, S., Potapchenko, N., Kosinova, V., Goncharuk, V., 2008. Adhesion of microorganisms to polymer membranes: a photobactericidal effect of surface treatment with TiO_2. Desalination 220, 380-385.

Leonard, B.P., 1979. A stable and accurate convective modelling procedure based on quadratic upstream interpolation. Comput Meth Appl Mech Eng 19, 59-98.

Menter, F.R., 1994. Two-equation eddy-viscosity turbulence models for engineering applications. AIAA J 32, 1598-1605.

Moreira, J.M.R., Araújo, J.D.P., Miranda, J.M., Simões, M., Melo, L.F., Mergulhão, F.J., 2014. The effects of surface properties on *Escherichia coli* adhesion are modulated by shear stress Colloid Surface B 123, 1-7.

Multanen, M., Talja, M., Hallanvuo, S., Siitonen, A., Välimaa, T., Tammela, T.L.J., Seppälä, J., Törmälä, P., 2000. Bacterial adherence to ofloxacin-blended polylactone-coated self-reinforced l-lactic acid polymer urological stents. BJU International 86, 966-969.

393 Nauman, E.A., Ott, C.M., Sander, E., Tucker, D.L., Pierson, D., Wilson, J.W., Nickerson, C.A.,
394 2007. Novel quantitative biosystem for modeling physiological fluid shear stress on cells. Appl
395 Environ Microbiol 73, 699-705.
396 Nikolaev, Y., Plakunov, V., 2007. Biofilm - "City of microbes" or an analogue of multicellular
397 organisms? Microbiology 76, 125-138.
398 Pace, J.L., Rupp, M.E., Finch, R.G., 2006. Biofilms, Infection and Antimicrobial Therapy. CRC
399 pres Taylor and Francis group, Boca Raton.
400 Petrova, O.E., Sauer, K., 2012. Sticky situations - Key components that control bacterial surface
401 attachment. J Bacteriol 194, 2413–2425.
402 Rivet, C., Lee, H., Hirsch, A., Hamilton, S., Lu, H., 2011. Microfluidics for medical diagnostics
403 and biosensors. Chem Eng Sci 66, 1490-1507.
404 Robert, J.M., Salek, M.M., 2010. Numerical simulation of fluid flow and hydrodynamic analysis
405 in commonly used biomedical devices in biofilm studies, in: Angermann, L. (Ed.), Numerical
406 Simulations - examples and applications in computational fluid dynamics. InTech, Canada, pp.
407 194-212.
408 Salta, M., Capretto, L., Carugo, D., Wharton, J.A., Stokes, K.R., 2013. Life under flow: A novel
409 microfluidic device for the assessment of anti-biofilm technologies. Biomicrofluidics 7, 0641181
410 - 06411816.
411 Shumi, W., Kim, S.H., Lim, J., Cho, K.-S., Han, H., Park, S., 2013. Shear stress tolerance of
412 S*treptococcus mutans* aggregates determined by microfluidic funnel device (μFFD). J Microbiol
413 Methods 93, 85-89.
414 Shunmugaperumal, T., 2010. Biofilm eradication and prevention: a pharmaceutical approach to
415 medical device infections. Wiley, New Jersey.

Simões, M., Simões, L.C., Cleto, S., Pereira, M.O., Vieira, M.J., 2008. The effects of a biocide and a surfactant on the detachment of *Pseudomonas fluorescens* from glass surfaces. Int J Food Microbiol 121, 335-341.

Situma, C., Hashimoto, M., Soper, S.A., 2006. Merging microfluidics with microarray-based bioassays. Biomolecular Engineering 23, 213-231.

Stoodley, P., Sauer, K., Davies, D.G., Costerton, J.W., 2002. Biofilms as complex differentiated communities. Annu Rev Microbiol 56, 187-209.

Teodósio, J.S., Simões, M., Melo, L., Mergulhão, F.J., 2013. Platforms for in vitro biofilm studies, in: Simões, M., Mergulhão, F.J. (Eds.), Biofilms in bioengineering. Nova science publishers pp. 45-61.

Teodósio, J.S., Simões, M., Melo, L.F., Mergulhão, F.J., 2011. Flow cell hydrodynamics and their effects on *E. coli* biofilm formation under different nutrient conditions and turbulent flow. Biofouling 27, 1-11.

Teodósio, J.S., Simões, M., Mergulhão, F.J., 2012. The influence of non-conjugative *Escherichia coli* plasmids on biofilm formation and resistance. J Appl Microbiol 113, 373–382.

Trautner, B.W., Darouiche, R.O., 2004. Role of biofilm in catheter-associated urinary tract infection. Am J Infect Control 32, 177-183.

van Oss, C., 1994. Interfacial Forces in Aqueous Media. Marcel Dekker Inc., New York, USA.

Weinstein, R.A., Darouiche, R.O., 2001. Device-associated infections: a macroproblem that starts with microadherence. Clinical Infectious Diseases 33, 1567-1572.

Wood, M., 1999. Conjunctivitis: Diagnosis and Management. Community Eye Health 12, 19-20.

Figure captions

Figure 1 Wall shear stress: a) in the bottom wall of the PPFC (*xy* plane) and b) in the bottom wall of the microchannel (*xy* plane).

Figure 2 Wall shear stress along the *x*-axis on the bottom wall of the microchannel (full line) and the PPFC (dotted line). The *x* position along the microchannel and the PPFC was normalized by the length, 15 and 256 mm, respectively.

Figure 3 Adhesion of *E. coli* on: a) PLLA, b) CA, c) PDMS and d) glass in the microchannel (open symbols) and in the PPFC (closed symbols) during 30 min. These results are an average of those obtained from three independent experiments for each surface and system. Time points represented with an * correspond to values where no statistical difference ($P > 0.05$) was found between the two platforms. Error bars represent the standard deviation from three independent experiments.

Figure 4 Bacterial adhesion rates on glass, PDMS, CA and PLLA obtained in the microchannel (black bars) and in the PPFC (white bars). Error bars shown for each surface represent the standard deviation from three independent experiments.

Table 1 Microchannel and PPFC dimensions, operational data and numerical results.

	Microchannel	**PPFC**
Section area / mm^2	0.045	128
Height scale factor	80x	
Aspect ratio	4.5	2.0
Flow rate / (mL.s^{-1})	2.0x10^{-5}	4

Average velocity / ($m.s^{-1}$)	$4.4x10^{-4}$	0.04
Average shear stress / Pa	0.022±0.002	
Maximum surface coverage / %	6.37±0.14	6.34±0.37

Table 2 Contact angle measurements of each surface (bacteria, PLLA, PDMS, CA, glass) with the three liquids, water (θ_w), formamide (θ_{form}) and α-bromonaphtalene (θ_{br}) and hydrophobicity (ΔG).

Surface	**Contact angle / º**			**Hydrophobicity/ ($mJ.m^{-2}$)**

	θ_w	θ_{form}	θ_{br}	ΔG
PLLA	88.0 ± 1.0	68.5 ± 0.9	25.6 ± 1.5	-65.3
PDMS	113.6 ± 0.6	111.2 ± 0.6	87.6 ± 1.8	-61.8
CA	65.2 ± 0.5	36.6 ± 2.0	22.5 ± 1.1	-36.0
Glass	16.4 ± 0.4	17.2 ± 0.4	44.5 ± 0.7	27.9
E. coli	19.1 ± 0.9	73.3 ± 0.7	58.5 ± 2.0	121.9

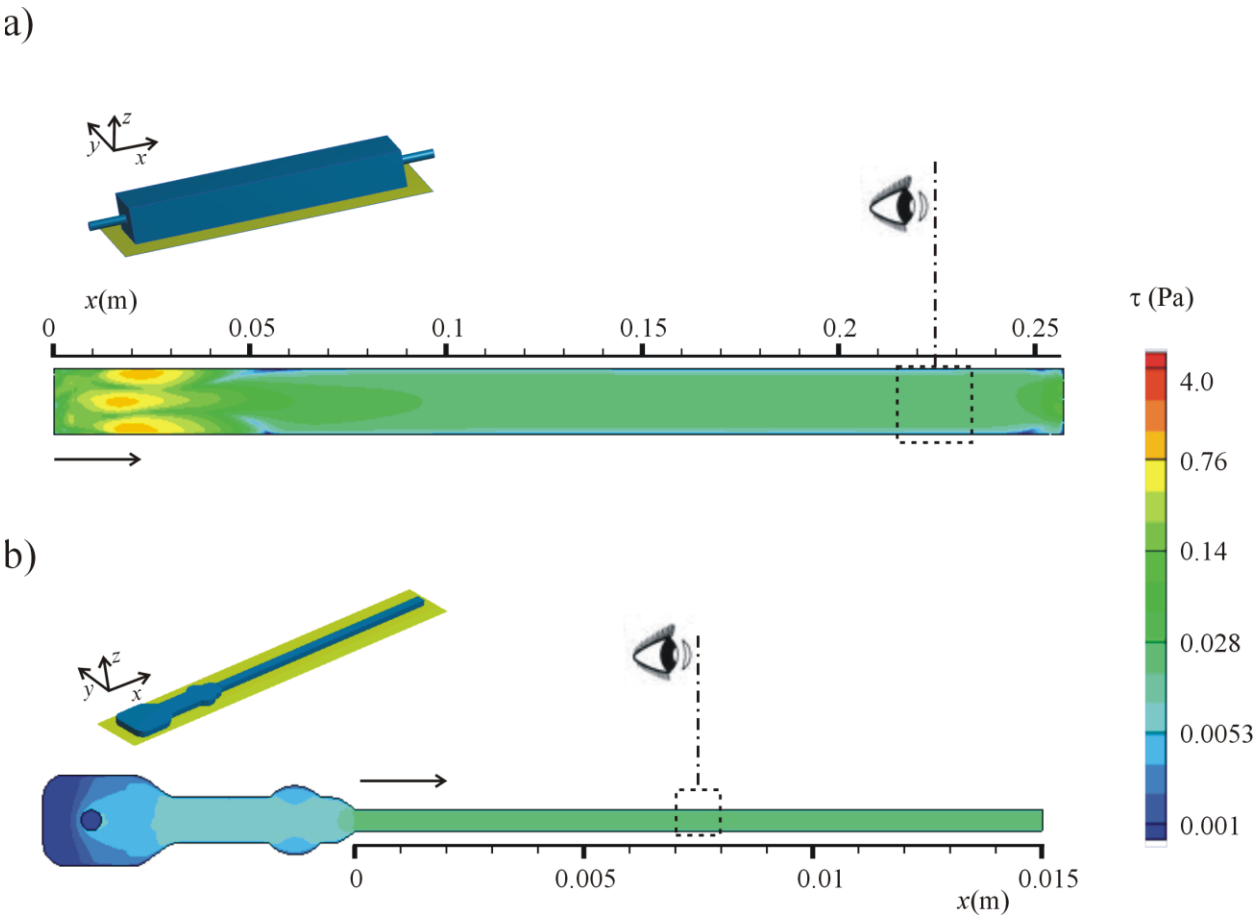

510

511 **Figure 1** Wall shear stress: a) in the bottom wall of the PPFC (*xy* plane) and b) in the bottom wall

512 of the microchannel (*xy* plane).

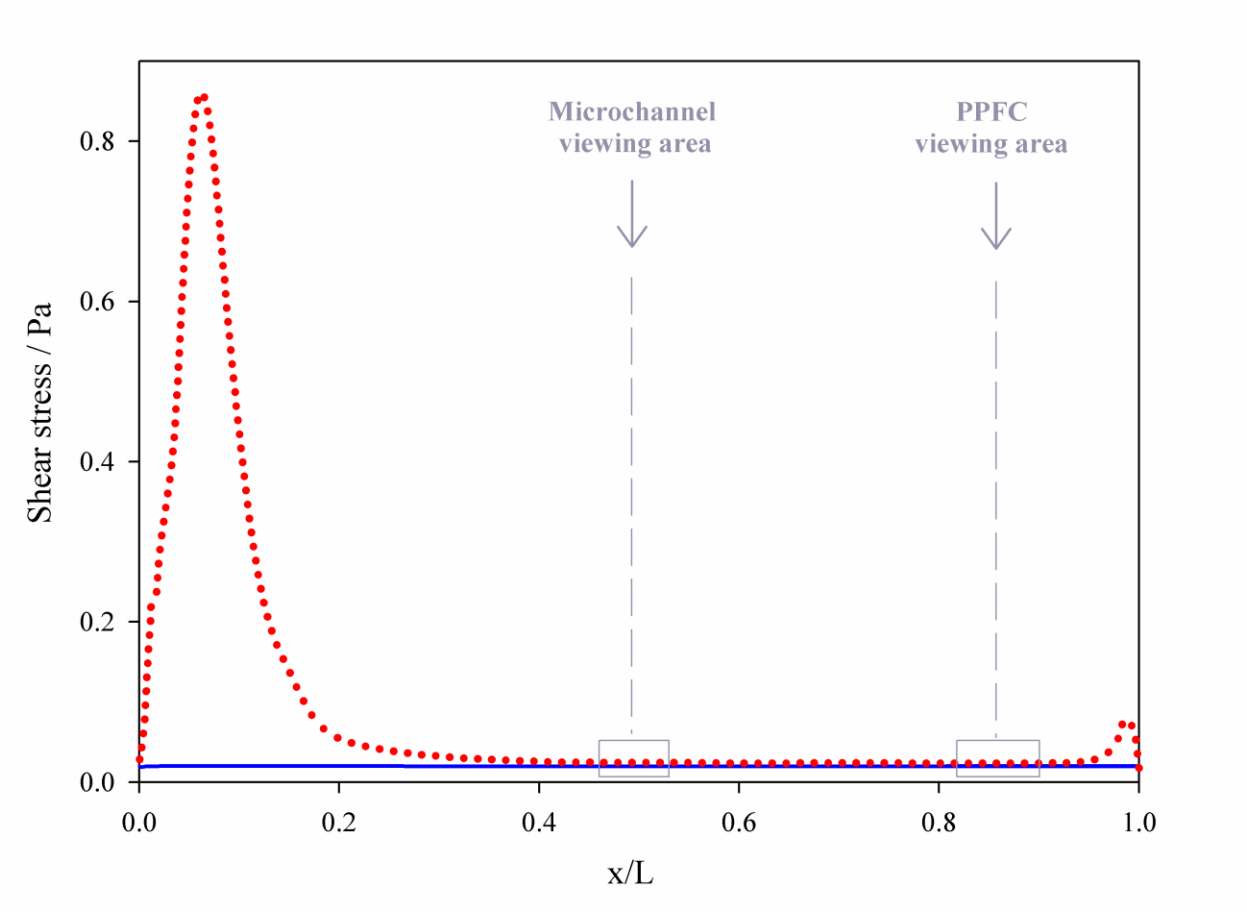

513

514 **Figure 2** Wall shear stress along the *x*-axis on the bottom wall of the microchannel (full line) and
515 the PPFC (dotted line). The *x* position along the microchannel and the PPFC was normalized by
516 the length, 15 mm and 256 mm, respectively.

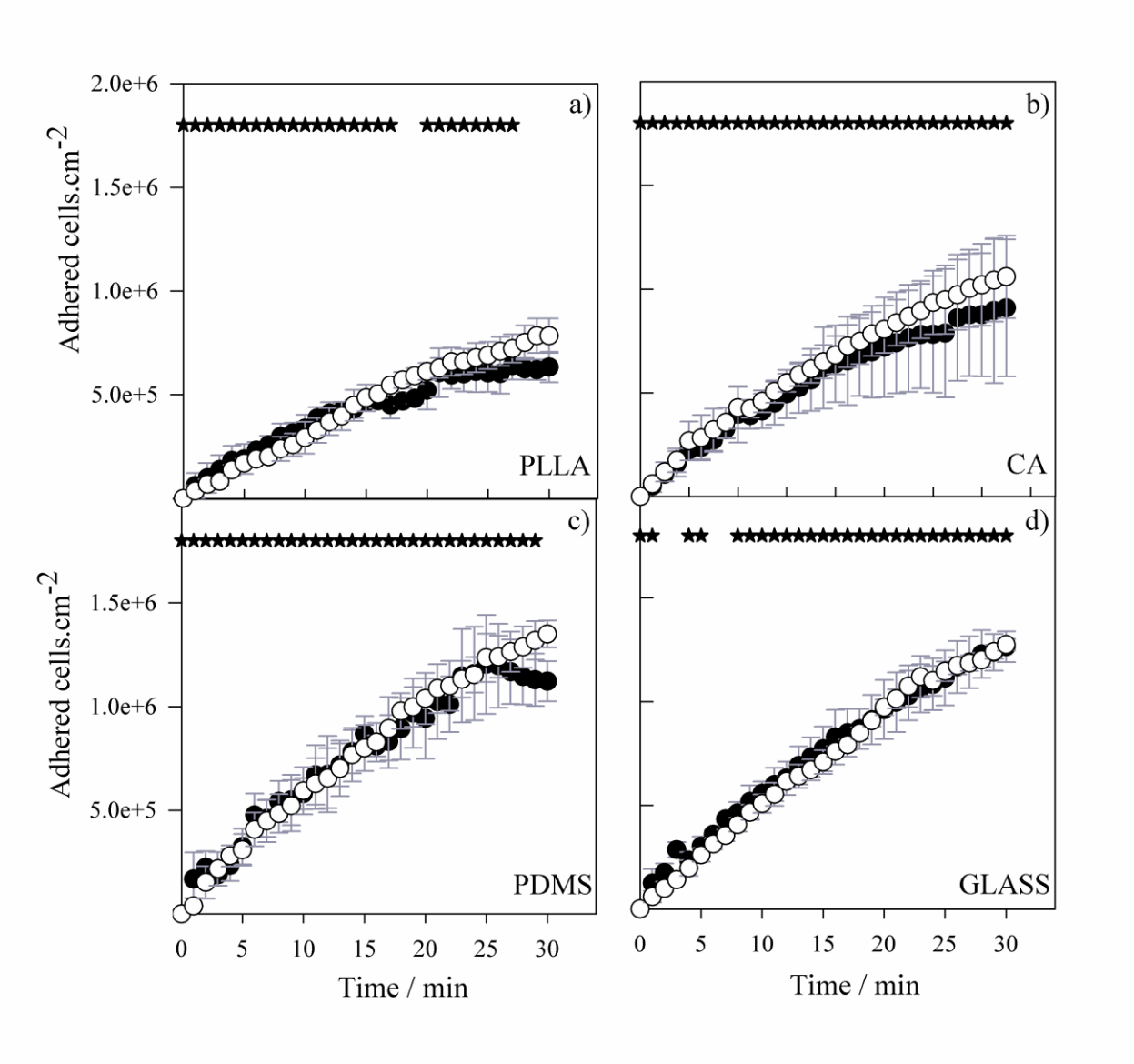

517

518 **Figure 3** Adhesion of *E. coli* on: a) PLLA, b) CA, c) PDMS and d) glass in the microchannel
519 (open symbols) and in the PPFC (closed symbols) during 30 min. These results are an average of
520 those obtained from three independent experiments for each surface and system. Time points
521 represented with an * correspond to values where no statistical difference ($P > 0.05$) was found
522 between the two platforms. Error bars represent the standard deviation from three independent
523 experiments.

524

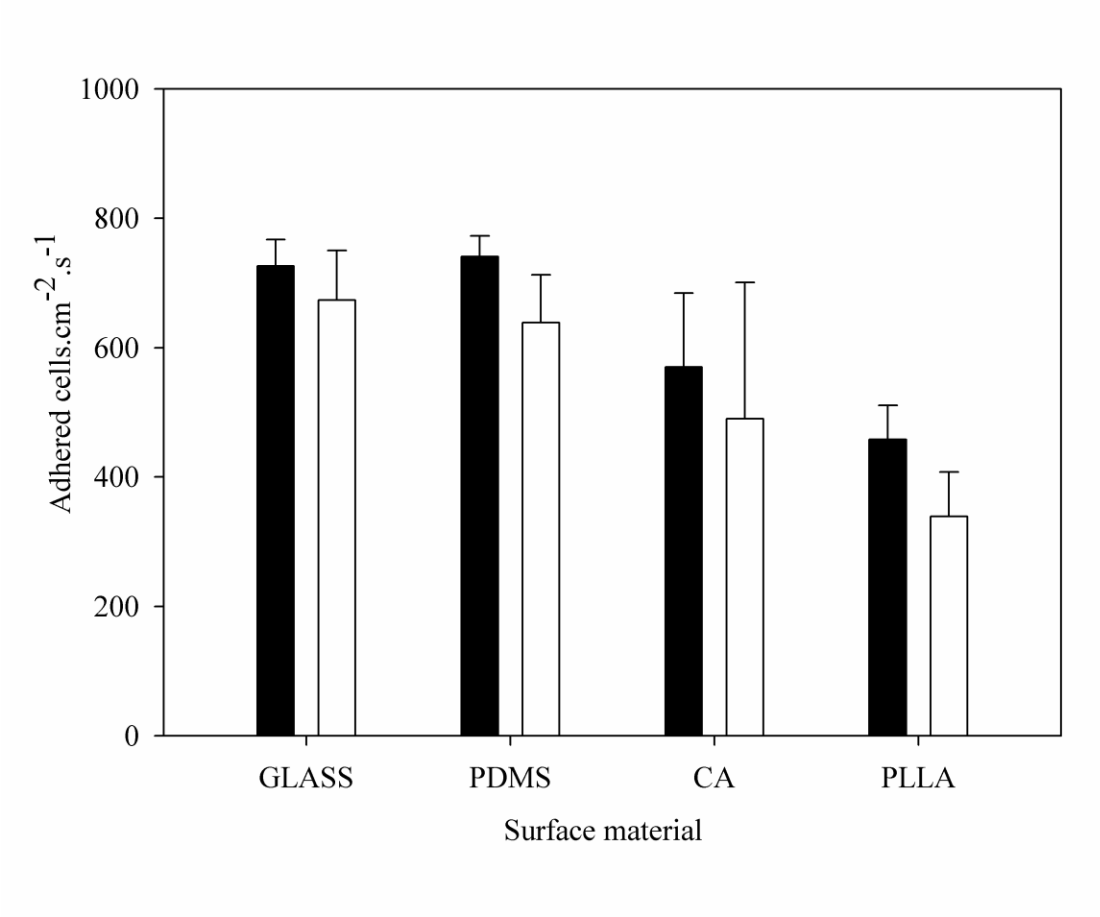

525

526 **Figure 4** Bacterial adhesion rates on glass, PDMS, CA and PLLA obtained in the microchannel
527 (black bars) and in the PPFC (white bars). Error bars shown for each surface represent the standard
528 deviation from three independent experiments.